

# Signal-to-noise optimization of medical imaging systems

Ian A. Cunningham

The John P. Robarts Research Institute and London Health Sciences Centre,  
100 Perth Drive, P.O. Box 5015, London, Ontario, Canada N6A 5K8,  
and

Rodney Shaw

Hewlett-Packard Research Laboratories, 1501 Page Mill Road, Palo Alto, California 94304

Over recent decades a quiet revolution has taken place in the application of modern imaging theory to many fields of applied imaging. Nowhere has this movement been more dramatic than within the field of diagnostic medical x-ray imaging, to the extent that there is now a growing consensus around a universal imaging language for the description and inter-comparison of the increasingly diverse range of technologies. This common language owes much to the basic quantum-limited approach pioneered by Rose and his contemporaries. It embodies the fundamentally statistical nature of image signals, and enables scientists and engineers to develop new system designs optimized for the detection of small signals while constraining patient x-ray exposures to tolerable levels. In this paper we attempt to provide a summary of some of the more salient features of progress being made in the understanding of the signal-to-noise limitations of medical imaging systems, and to place this progress within historical context. Reflecting the experiences of both authors, emphasis will be given to medical diagnostics based on x-ray imaging techniques.

## I. INTRODUCTION

Both the complexity and sophistication of medical imaging systems have increased dramatically over the past several decades. Alongside this development there has been a progression in the knowledge of the fundamental relationships that govern image quality in these systems, many of which can be traced directly to the pioneering work of Albert Rose. This has facilitated the identification of key metrics that can be used to compare different imaging technologies, and the development of predictive theories and models that can be used in the design of new systems. In earlier days, attention was initially focused on what might be described as “mean-level” relationships between the input and output of an imaging system. For instance, it was determined that the sensitometric properties of radiographic film-screen systems could be expressed in terms of a characteristic curve - sometimes referred to as an H & D (Hurter and Driffeld) curve - relating film optical density to x-ray exposure. As insight came to these important mean-level relationships, practical control and technical-standards followed.<sup>1</sup> At the same time there was also a growing realization that further progress was dependent on an improved understanding of the higher-order relationships between input and output, including the transfer of statistical fluctuations, or noise, and the reproduction of fine spatial detail.

This article describes some aspects of the development of *transfer theory*, as it has come to be known, from the early photon-counting work of Albert Rose quantifying fundamental image-noise limitations for the first time, through the development by Shaw and his contemporaries of spatial-frequency dependent metrics including the noise-equivalent number of quanta (NEQ) and detective quantum efficiency (DQE), to our current understanding of more generalized

signal- and noise-transfer relationships in complex systems. These latter relationships, developed within the context of medical diagnostic imaging over the past decade by Rabbani, Shaw and Van Metter and discussed in more detail below, provided an important link between the early Rose approach and modern linear-systems theories. In its simplest form, the term *signal transfer* has come to mean the description of the transfer of spatial detail in the signal from the input to the output of an imaging system, while *noise transfer* relates to the corresponding noise attributes. Both are expressed in terms of a spatial-frequency-dependent analysis in which imaging systems are described as *stochastic linear systems*. Together they are now used for the description of image quality in terms of the NEQ, and system performance in terms of the DQE and frequency-dependent quantum sinks.

## II. IMAGE QUALITY: ROSE MODEL TO NEQ

### A. Rose Model

The stochastic nature of image quanta imposes a fundamental limitation on the performance of photon-based imaging systems. This was first recognized in 1948 by Rose<sup>2,3</sup> and his contemporaries,<sup>4-6</sup> and their work forms the basis of many introductory descriptions of signal and noise in radiography. Rose demonstrated this relationship with a series of pictures<sup>7</sup> that in many ways symbolize his seminal contributions to the medical imaging community and are reproduced in the introduction to this special issue. They show an image acquired with varying numbers of optical image quanta. As more quanta are used, image quality improves and finer detail can be resolved.

The relationship between the number of image quanta and perception of detail is embodied in the ‘‘Rose Model,’’ as it has come to be known, that describes the signal-to-noise ratio (SNR) for the detection of a uniform object of area  $A$  in a uniform background having a mean  $\bar{q}_b$  quanta per unit area. If  $\bar{q}_o$  is the mean number of quanta per unit area in the region of the object, the resulting contrast can be written as  $C = (\bar{q}_b - \bar{q}_o)/\bar{q}_b$ . Rose defined signal to be the incremental change in the number of image quanta due to the object,  $A(\bar{q}_b - \bar{q}_o)$ , and noise to be the standard deviation in the number of quanta in an equal area of uniform background,  $\sigma_b$ . For the special case of uncorrelated background quanta, noise is described by Poisson statistics and  $\sigma_b = \sqrt{A\bar{q}_b}$  so that the Rose SNR,  $SNR_{Rose}$ , is given by

$$SNR_{Rose} = \frac{A(\bar{q}_b - \bar{q}_o)}{\sqrt{A\bar{q}_b}} = C\sqrt{A\bar{q}_b}. \quad (1)$$

Rose showed that  $SNR_{Rose}$  must have a value of approximately five or greater for reliable detection of an object. Implications and limitations of the Rose model are described in terms of modern detection theory by Burgess<sup>8</sup> elsewhere in this special issue.

The Rose model played an essential role in establishing the fact that image quality is ultimately limited by the statistical nature of image quanta. However, its limitations quickly become apparent when used to assess image quality in many practical situations. The primary restriction was the definition of noise used by Rose in Eq. (1) that is valid *only* for a statistically uncorrelated distribution of image quanta. Estimates of noise based on measured image data for use in the Rose model may be erroneously high or low as affected by a number of factors, including the presence of additive system noise (e.g. electronic or film noise) and in particular statistical correlations in the image data. These correlations may be introduced by scatter of x rays or secondary quanta in the detector system (e.g. light in a radiographic screen), and will affect image appearance. For these reasons, the original Rose model needs appropriate extension and elaboration to be of practical value in the analysis of most modern medical imaging systems.

## B. Communication-Theory Based Approach

The pursuit of a more complete understanding of image quality and system performance required the development of a theory that incorporated second-order image statistics, and would therefore be sensitive to statistical correlations in image data. Specifically, these problems called for a general communication-theory based approach. The various crucial components of this theory were already substantially in place, the first and most obvious being the Fourier-transform linear-systems approach.

### 1. Signal Transfer: The Modulation-Transfer Function

The Fourier transform has been used extensively in many areas of study, including engineering and communication

fields for the analysis of time-varying signals, and optical science in the development of Fourier optics. During the 1960s, Rossmann, Doi and co-workers<sup>9-14</sup> were largely responsible for adapting these concepts for use by the medical-imaging community, enabling a quantitative description of signal-transfer relationships. The Fourier transform was used to express spatially-varying signals (i.e. images) in medical systems in terms of spatial frequencies (cycles/mm),  $u$ . The effect of image-blurring mechanisms were represented both as two-dimensional convolution integrals with a point-spread function (PSF) in the spatial domain, and as multiplicative transfer functions in the spatial-frequency (Fourier) domain. Sinusoidal image patterns are transferred with only a scalar change in amplitude, and Rossmann and his contemporaries expressed these factors as a spatial-frequency dependent ‘‘modulation-transfer function’’ (MTF).<sup>15</sup> Sinusoidal functions were thus identified as being the eigenfunctions of imaging systems while the MTF described the eigenvalues. By definition, the MTF is normalized to unity at  $u = 0$ .

With this notation, it became possible to separate the influence of various image-blurring mechanisms from the overall system MTF, including the influence of x-ray source focal-spot shape (Doi,<sup>10</sup> Burgess<sup>16,17</sup>) and radiographic-screen blur (Rossmann,<sup>9</sup> Metz & Doi<sup>18</sup>). General works describing the application of linear-systems analysis have subsequently been published by various authors including Gaskill.<sup>19</sup> Specific application to radiographic imaging has been described by Dainty & Shaw<sup>20</sup> and Metz & Doi<sup>18</sup> among others. Perhaps the most extensive use of linear-systems theory in the medical imaging field is described by Barrett & Swindell,<sup>21</sup> who used this approach to describe fundamental principles and characteristics of many imaging systems in radiography, computed tomography (CT), nuclear medicine, ultrasound and other areas. Use of the MTF is less established in magnetic resonance imaging (MRI), but may have a significant role to play.<sup>22</sup>

## 2. Linear and Shift-Invariant System Response

Use of the Fourier-based approach requires that two important conditions be satisfied.<sup>18</sup> The first requires the system to have a linear response to an input stimulus. Essentially, this means the output must be proportional to the input. The second condition requires the system to have a shift-invariant response. That is, any blurring mechanism must apply equally to all regions of an image. Systems satisfying both conditions are sometimes referred to as linear and shift-invariant (LSI) systems. Systems displaying only small-signal linearity (such as film-screen systems), or only local shift invariance (such as x-ray image-intensifier systems), can often be modeled using the linear-systems approach if reasonable practical approximations are made.

## 3. Image Signals

The transfer-theory approach is based on specific input-output relationships. In this context, the output may be an exposed film, or a digital image described in terms of a two-dimensional array of (unitless) numerical values, and the

input may be a distribution of x-ray quanta (quanta/mm<sup>2</sup>) requiring that principles of distribution theory<sup>19</sup> be incorporated into the transfer relationships. In this article,  $q(x, y)$  is used to represent a sample function of the random process generating the input distribution. Physical measurements of the distribution  $q(x, y)$  require the use of a *sampling function*, or measurement function,<sup>19</sup> and will be represented as  $d(x, y)$ .

#### 4. The (Wiener) Noise-Power Spectrum

As linear-systems theory was advanced within the medical imaging community, it was found, as in other fields of applied imaging, that once the intellectual barrier of visualizing input-output relationships in the spatial-frequency domain rather than the spatial domain was overcome, there were substantial physical insights to be gained in the analysis of increasingly complex systems. At the same time, and with the practical interest often being in the limitations of quantum-limited imaging tasks, there was a growing realization that there was a parallel need for the Rose<sup>2,3,7,23,24</sup> approach. While absolute noise measurements on rare-earth intensifying screens had been reported in the early seventies,<sup>25</sup> and the work of Rose and the advantages of the noise-equivalent approach were well-known within the medical imaging community having been introduced by Schade<sup>26</sup> and others, these concepts were often applied with a separate context having little or no overlap with the linear-systems viewpoint.

As mentioned above, the Rose model described noise in terms of the statistical variance in a number of uncorrelated quanta in a specified area  $A$ . This was found to be inadequate when noise was estimated from real image data primarily because it did not properly treat the influence of spatial correlations in the noise. To overcome this, second-order statistical correlations were incorporated by specifying the mean and auto-covariance of the noise process. Adopting the Fourier-based notation of the linear-systems approach, noise in a uniform image described by the stationary ergodic random process (these terms are defined below)  $d(x, y)$  was expressed in terms of the noise-power spectrum (NPS) or Wiener spectrum,  $NPS_d(u, v)$ , given both as the Fourier transform of the auto-covariance of  $d(x, y)$ ,<sup>27</sup>  $NPS_d(u, v) = F\{K_{dd}(x, y)\}$ , and as<sup>20</sup>

$$NPS_d(u, v) = \lim_{X, Y \rightarrow \infty} E \left\{ \frac{1}{2X} \frac{1}{2Y} \left| \int_{-X}^X \int_{-Y}^Y \Delta d(x, y) e^{-i2\pi(ux+vy)} dx dy \right|^2 \right\} \quad (2)$$

where  $E\{ \}$  is the expectation operator,  $\Delta d(x, y) = d(x, y) - E\{d(x, y)\}$ , and  $u$  and  $v$  are spatial frequencies in the  $x$  and  $y$  directions respectively. It is often more convenient to express the NPS in one dimensional geometry rather than two, generally as  $NPS_d(u) = NPS_d(u, v)|_{v=0}$ . It will also be noticed from Eq. (3) that the units of  $NPS_d(u, v)$  are equal to those of  $d^2(x, y) \times x \times y$ . Therefore, the NPS of a dimensionless signal such as a pixel value in a digital image, or optical density, will typically have the units mm<sup>2</sup> or mm in two dimensions or one respectively, while the NPS of a distribution of quanta will typically have the units mm<sup>-2</sup> or mm<sup>-1</sup>.

The link to the Rose model is made by first noting that the variance is related to the NPS by<sup>27</sup>

$$\sigma^2 = \int_{-\infty}^{\infty} \int_{-\infty}^{\infty} NPS(u, v) dudv. \quad (3)$$

The distribution of background quanta can be represented as the sample function  $q_b(x, y)$  consisting of spatially-distributed  $\delta$ -functions where each  $\delta$ -function represents a quantum.<sup>21</sup> The number of background quanta in a rectangular region  $A$ ,  $N_b$ , is then given by

$$N_b = \int_{-a_x/2}^{a_x/2} \int_{-a_y/2}^{a_y/2} q_b(x, y) dx dy \quad (4)$$

$$= \int_{-\infty}^{\infty} \int_{-\infty}^{\infty} q_b(x, y) \Pi \left( \frac{x}{a_x}, \frac{y}{a_y} \right) dx dy \quad (5)$$

where we have let the sampling function coincide exactly with the rectangular region  $A$ . This result can also be expressed as the convolution of  $q_b(x, y)$  with  $\Pi(x/a_x, y/a_y)$  evaluated at  $x, y$  corresponding to the center of  $A$  giving

$$N_b = q_b(x, y) ** \Pi(x/a_x, y/a_y)|_{x,y=0,0} \quad (6)$$

$$= d(x, y)|_{x,y=0,0} \quad (7)$$

where  $**$  represents the two-dimensional convolution operation and  $d(x, y)$  is a function that, when evaluated at some position  $x, y$ , gives the number of quanta in the rectangular region  $A$  centered at that location. Since  $q_b(x, y)$  describes a stationary ergodic random process,  $d(x, y)$  also describes a stationary ergodic random process. Therefore, the variance of  $d(x, y)$  equals that of  $N_b$  which are samples of  $d(x, y)$ , and the convolution theorem can be used to show<sup>28</sup>

$$\sigma_b^2 = \int_{-\infty}^{\infty} \int_{-\infty}^{\infty} NPS_d(u, v) dudv \quad (8)$$

$$= a_x^2 a_y^2 \int_{-\infty}^{\infty} \int_{-\infty}^{\infty} NPS_b(u, v) \text{sinc}^2(\pi a_x u) \text{sinc}^2(\pi a_y v) dudv \quad (9)$$

where  $NPS_d(u, v)$  and  $NPS_b(u, v)$  are the NPS of  $d(x, y)$  and  $q_b(x, y)$  respectively. When  $q_b(x, y)$  describes uniformly distributed uncorrelated quanta,  $NPS_b(u, v) = \bar{q}_b$  for all frequencies, giving

$$\sigma_b^2 = a_x^2 a_y^2 \bar{q}_b \int_{-\infty}^{\infty} \int_{-\infty}^{\infty} \text{sinc}^2(\pi a_x u) \text{sinc}^2(\pi a_y v) dudv \quad (10)$$

$$= a_x a_y \bar{q}_b = A \bar{q}_b \quad (11)$$

which is the Rose noise used in Eq. (1).

This example illustrates a specific case where the Rose result is equivalent to the more general Fourier-based result. In general, however, the Rose method must be used with care as misleading results are obtained when image quanta are statistically correlated, or when the sampling function - that would normally be the PSF of the system - does not correspond exactly with the size and shape of the object  $A$ . It is then necessary that the variance be expressed in terms of the integral of Eq. (8) where the background image NPS is weighted by the (squared) Fourier components of the desired object shape before being integrated over all spatial frequencies. *In other words, noise variance is tied to both the object*

shape and system sampling function, and cannot be stated independently. Only if the object dimensions  $a_x$  and  $a_y$  are large with respect to the correlation distances, so that the sinc-functions are sufficiently narrow that they extend only over a small frequency range in which the NPS is approximately uniform, does the variance become independent of object shape and the Rose method give an accurate measure of noise.

Measurement of the NPS remains a complex subject. In an effort to provide guidelines and recommendations, the American Association of Physicists in Medicine formed the Task Group on Standards for Noise Power Spectra Analysis (Task Group #16, report pending) in 1994 to help standardize methods of measuring and reporting results.

### 5. Stationary Ergodic Random Processes

Use of Fourier-based descriptions of image noise requires two important assumptions.<sup>20,27</sup> The first is that processes responsible for noise both in the input signal and within the imaging chain be wide-sense stationary (WSS). This means that the mean and auto-covariance of the noise processes, and the second-order noise-transfer characteristics of the system, are the same in all regions of the image, a condition often satisfied for the analysis of noise in low-contrast imaging tasks. The second assumption is that the system be ergodic which means that statistics that should really be determined from ensemble averages of many image realizations can be determined from the statistics of a single realization (a single image). While it can be difficult to prove ergodicity, many systems of practical importance are approximately ergodic.

### 6. Noise-Equivalent Quanta, NEQ

The critical need for bridging the seemingly distinct Rose-based particle approach and the Fourier-based wave approach came with the practical problem of absolute scaling of signal- and noise-power spectra. Results obtained using Eq. (3) are expressed in output units which may be arbitrary or specific to a particular imaging system. By expressing image noise in terms of the number of Poisson-distributed input photons per unit area at each spatial frequency, Shaw obtained a common *absolute* scale of noise - the noise-equivalent number of quanta (NEQ).<sup>20,29</sup>

The NEQ of linear imaging systems is given by

$$NEQ(\bar{q}, u) = \frac{\bar{q}^2 \bar{G}^2 MTF^2(u)}{NPS_d(u)} \quad (12)$$

$$= \frac{\bar{d}^2 MTF^2(u)}{NPS_d(u)} \quad (13)$$

where  $\bar{q}$  is the (uniform) average number of input quanta per unit area,  $\bar{G}$  is the scaling factor relating  $\bar{q}$  to the average output  $\bar{d}$ , and  $NPS_d(u)$  is the output NPS. The units of NEQ are the same as those of  $\bar{q}$ . Equation (13) is particularly convenient to use in many practical situations as it only requires the terms  $\bar{d}$ ,  $MTF(u)$ , and  $NPS_d(u)$ , all of which are readily determined experimentally from measured image data. Film-screen systems have a non-linear response to x-ray exposure, and exhibit only small-signal linearity. The

NEQ is therefore given by<sup>20</sup>

$$NEQ(\bar{q}, u) = \frac{(\log_{10} e)^2 \gamma^2 MTF^2(u)}{NPS(u)} \quad (14)$$

where  $\gamma$  is the slope of the characteristic optical density versus log-exposure curve corresponding to the same exposure level as the NPS measurement.

The NEQ concept is attractive as it expresses image quality on an absolute scale - the number of equivalent Poisson-distributed input quanta. It can be measured for specific systems at specified exposure levels in various laboratories and the results can be directly compared. An image with a greater NEQ corresponds to lower image noise. An excellent description of the NEQ in terms of modern detection theory is available as an ICRU report.<sup>30</sup>

## III. QUANTIFYING SYSTEM PERFORMANCE

In spite of these and other early contributions, in the medical imaging community it was not until the mid-eighties that the application of modern SNR-based theory to imaging progressed from an occasionally interesting fringe activity to a core topic providing a universal language. Since that time, the number of publications in this area has grown tremendously, certainly too many to fully acknowledge here.<sup>30,31</sup> In the following, we attempt to summarize some of this development with examples and illustrations that reflect the mutual interests of the authors.

### A. Signal-to-Noise Ratio, SNR

In the Fourier-based analysis, signal is described as the modulation of a sinusoidal signal. Thus, the Fourier-based description of the signal-to-noise ratio (SNR) at a specified exposure level is determined by

$$SNR^2(\bar{q}, u) = \frac{\bar{d}^2 MTF^2(u)}{NPS_d(u)} = NEQ(\bar{q}, u) \quad (15)$$

showing that in the Fourier-based analysis, the SNR is equal to the square root of the effective number of Poisson-distributed quanta, i.e.  $SNR(\bar{q}, u) = \sqrt{NEQ(\bar{q}, u)}$ , analogous to the particle relationship used by Rose where  $SNR = \sqrt{N}$ .

### B. Detective Quantum Efficiency, DQE

It was further realized that the absolute scaling of system-performance metrics was greatly facilitated by the introduction of the Rose-based concept of detective quantum efficiency (DQE). Whereas this arose in a discrete (photon-counting) context, it was readily extended to be compatible with Fourier concepts by the introduction of a fuller definition in terms of spatial-frequency power spectra. Specifically, it was shown<sup>29</sup> that the DQE of a linear imaging system could be written as

$$DQE(u) = \frac{NEQ(u)}{\bar{q}} = \frac{\bar{q} \bar{G}^2 MTF^2(u)}{NPS_d(u)} \quad (16)$$

$$= \frac{\bar{d}^2 MTF^2(u)}{\bar{q} NPS_d(u)} \quad (17)$$

which, in the absence of additional noise sources, is independent of  $\bar{q}$ . The DQE is closely related to the NEQ, but rather than expressing the effective number of Poisson-distributed input quanta, it is normalized to express the fraction of input quanta used to create an image at each spatial frequency. Thus, while the NEQ is a metric describing image quality and is generally dependent on  $\bar{q}$ , the DQE describes the ability of a particular imaging system to effectively use all available input quanta. An ideal imaging system has a DQE of unity. No system can have a DQE greater than unity.

The DQE has been described in a number of different but consistent forms. For instance, Eq. (17) is particularly useful for experimentally determining the DQE of particular systems<sup>32</sup> although it can be difficult to obtain an accurate measure of the input  $\bar{q}$  for diagnostic x-ray spectra that consist of a wide range of energies. Additional details of this challenge have been described elsewhere.<sup>28</sup> For the special case when input quanta are uncorrelated and photon noise is the only significant source of input noise, the input squared SNR is  $SNR_{in}^2(u) = \bar{q}^2/NPS_q(u) = \bar{q}$ . The output squared SNR is  $\bar{d}^2 MTF^2(u)/NPS_d(u)$  and in this special case the DQE can be interpreted as the squared-SNR transfer relationship

$$DQE(u) = \frac{SNR_{out}^2(\bar{q}, u)}{SNR_{in}^2(\bar{q}, u)}. \quad (18)$$

However, as we shall see for non-radiation limited inputs and for multistage analyses, this interpretation must be used with caution as the DQE of a cascaded system is generally not a multiplicative cascade of DQEs.

The DQE of a film-screen based system is given by

$$DQE(\bar{q}, u) = \frac{(\log_{10} e)^2 \gamma^2 MTF^2(u)}{\bar{q} NPS(u)} \quad (19)$$

and is dependent on  $\bar{q}$  due to its non-linear response.

During the mid-seventies, metrics based on DQE were gradually introduced in an attempt to clarify such absolute scaling problems across a variety of medical imaging technologies<sup>33,34</sup> with Wagner and co-workers<sup>30,34</sup> deserving much of the credit for championing the widespread application of the noise-equivalent approach and providing some of the first absolute sets of DQE measurements.

## 1. DQE analysis of screen-film systems

During the mid-eighties, a series of publications<sup>35-40</sup> considered a new comprehensive model for radiographic film-screen imaging systems. This work also described a set of absolute experimental DQE and NEQ values made possible by carrying practical estimates of the Wiener spectrum of the image noise-power in order to carry out the absolute scaling required. An important aspect of the new model was that it combined the principal imaging components of screen and film systems separately into an overall DQE expression that typically reduced to the form<sup>35</sup>

$$DQE_{SF}(\bar{q}, u) = \frac{\eta_S}{1 + \frac{\epsilon_m}{m} + \frac{1}{m\eta_F DQE_F(\bar{q}, u) MTF_S^2(u)}} \quad (20)$$

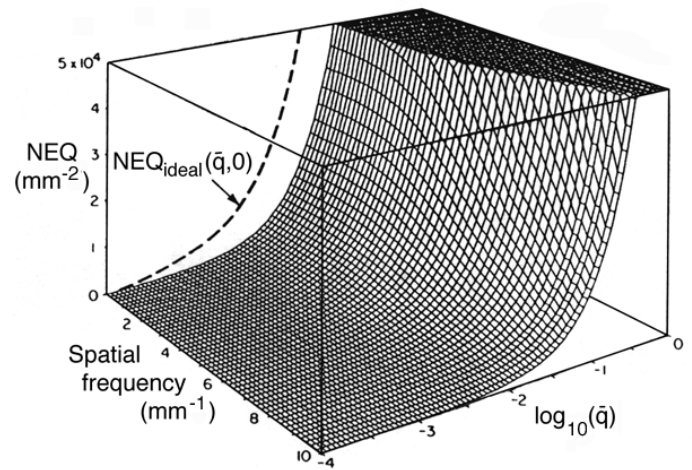


Figure 1: NEQ characteristics for a model screen,<sup>38</sup> compared with an ideal quantum-limited detector,  $NEQ_{ideal}(\bar{q}, 0)$ .

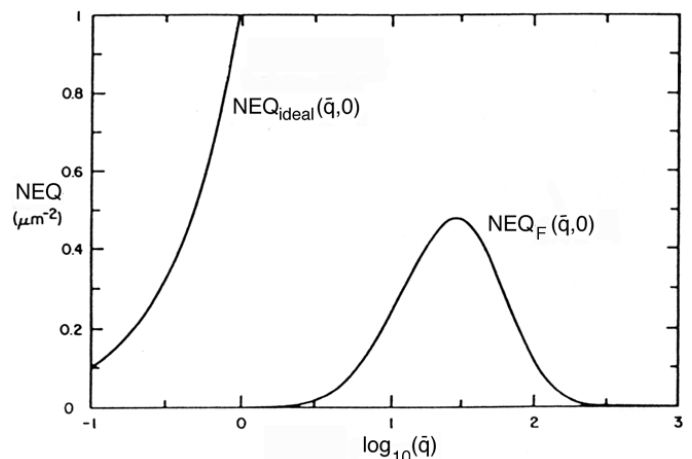


Figure 2: The low-spatial frequency NEQ characteristics for a model film.<sup>38</sup>

where  $\eta_S$  is the quantum efficiency of a screen having an optical conversion quantum gain  $m$ ,  $\epsilon_m$  is the Poisson excess in the gain that is related to the variance  $\sigma_m^2$  by  $\epsilon_m = \sigma_m^2/m - 1$  and reflects the fact that conversion from x rays to light is a random process,  $\eta_F$  is the coupling efficiency of light to the film,  $DQE_F(\bar{q}, u)$  is the DQE associated with the film alone, and  $MTF_S(u)$  is the MTF associated the screen alone. This model assumes a “thin” screen, neglecting variable x-ray interaction depths in the phosphor.

An important aspect of this model<sup>35,36,38</sup> was that it provided the first basis for the comparison of practical measurements of system DQE and those predicted from component values, and demonstrated a satisfactorily high degree of agreement.<sup>37,39</sup> Equation (20) has subsequently been of use in establishing a broad understanding of the separate roles of the screen and film, and the manner in which their combinations may be optimized. It showed that the DQE is proportional to the quantum efficiency of the screen, and that a poor film DQE can be compensated for with a large optical conversion factor  $m$ . Figures 1 to 3 give an example of such combinations, demonstrating the predictive power of

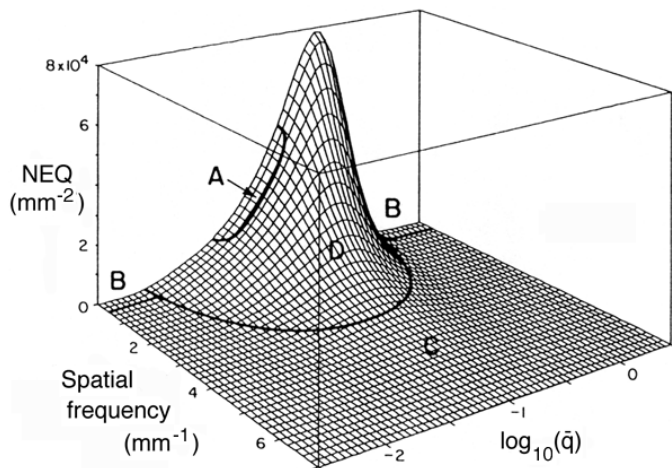


Figure 3: Model NEQ characteristics for screen-film combination. Regions A to D indicate differing influences of screen and film component parameters.

the model. Figure 1 shows the NEQ associated with the screen detection process as a function of both  $\bar{q}$  and spatial frequency,  $u$ . The ideal characteristics (the Rose quantum-limit),  $NEQ_{ideal}(\bar{q}, 0)$ , are also shown for comparison. Figure 2 shows the low spatial-frequency NEQ characteristics of the film. Finally, Fig. 3 shows the modeled NEQ characteristics of screen-plus-film. In region A the screen-film combination approximates to that of the screen alone, but at the very low and very high exposures the low-frequency NEQ (region B) will be that of the film alone. In region C the NEQ approximates the product of that of the film with that of the square of the transfer function (MTF) of the screen, while within region D all three factors (the NEQs of both screen and film and the screen transfer function) are significant in determining the output NEQ.

#### IV. GENERALIZED SIGNAL- AND NOISE-TRANSFER THEORY

A byproduct of this renewed interest in signal-to-noise transfer limitations was the realization that film-screen systems could be modeled as a serial cascade of simple amplifying and scattering processes,<sup>41</sup> and that expressions for both the signal- and noise-transfer characteristics of each process could be written in a simple closed form. This led directly to the development of a more generalized model of cascaded imaging systems, and this generalized model has subsequently been used to describe a wide range of modern digital and non-digital medical imaging systems. Because of these general signal- and noise-transfer implications, a brief summary will be given here.

##### A. Elementary Processes

Use of the generalized transfer approach to model complex systems as a serial cascade of simple amplification and scattering stages was an important step in the development of SNR-related concepts. It allowed the analysis of complex systems to be separated into more manageable components.

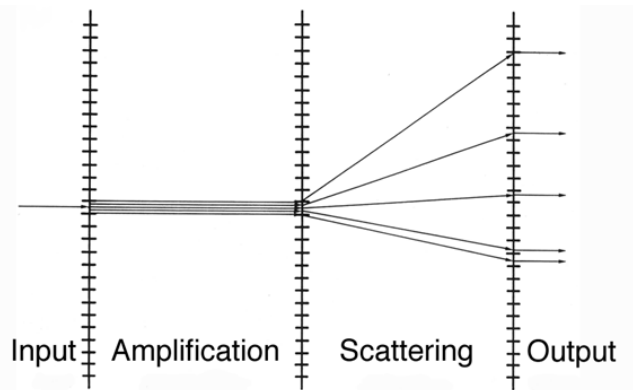


Figure 4: Schematic illustration of a stochastic amplification stage cascading into a stochastic scattering stage.<sup>41</sup>

The cascaded model was physically intuitive, and provided a solid theoretical framework from which a rigorous mathematical analysis could be developed. Rabbani, Shaw and Van Metter<sup>42,43</sup> pioneered the cascaded approach in a number of early studies using a multi-variate moment-generating analysis to determine the transfer characteristics of relatively complex systems. This allowed the statistical properties in the output image to be described in terms of the variance and auto-covariance in the input distribution of image quanta. They also showed that for the important case of wide-sense stationary noise processes required for any Fourier-domain analysis, the output image noise could also be described in terms of the spatial-frequency dependent noise-power spectrum. This offered an additional simplification since the signal and noise power transfer through a complex system could be determined by cascading simple transfer expressions for each elementary stage. Figure 4 illustrates the elementary processes of amplification and scattering, and Table 1 provides a summary of the transfer characteristics associated with each.

##### 1. Stochastic Amplification

Stochastic amplification<sup>42</sup> represents the process where each quantum in a distribution is converted into  $g$  quanta where  $g$  is a random variable that may assume only positive values and has a mean  $\bar{g}$  and variance  $\sigma_g^2$ . Noise-power transfer as shown in Table 1 is essentially a Fourier-based generalization of an earlier particle-based result described by Zwieg<sup>44</sup> in the mid-sixties. He described the DQE for a multi-stage quantum detector with gain and showed that

$$\sigma_{out}^2 = \bar{g}^2 \sigma_{in}^2 + \sigma_g^2 \bar{N}_{in}. \quad (21)$$

Stochastic amplification stages can also be used to describe the random selection (random loss) of events such as the quantum efficiency of a detector. In that case,  $g$  is a random variable with a value 0 or 1 only, an average  $\bar{g} \leq 1$ , and a variance given by<sup>21</sup>

$$\sigma_g^2 = \bar{g}(1 - \bar{g}). \quad (22)$$

Stochastic amplification of photon noise by one stage may produce a structure that constitutes effective signal to the

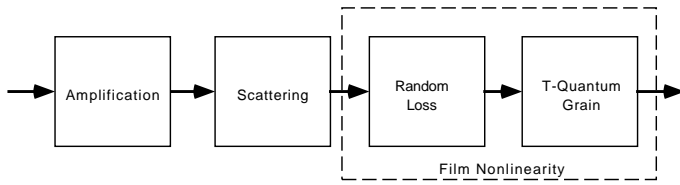


Figure 5: Schematic of the approach used to find a solution for noise transfer by a radiographic screen-film system.<sup>46,47</sup>

next stage, and thus it is essential to cascade these components in the proper way at each amplifying and scattering stage.

## 2. Stochastic Scattering

Stochastic scattering represents the process of randomly relocating each quantum in a distribution according to a specified PSF. It is thus a translated point process and has been called a stochastic mislocation process.<sup>45</sup> Analysis of the scattering stage<sup>42</sup> demonstrated that while by definition the signal structure (or modulation) is transferred via the MTF, photon noise is essentially unmodulated signal and as such bypasses the MTF of that stage as shown in Table 1 where  $MTF(u)$  is the scatter MTF.

## 3. Deterministic Blur

Also shown in Table 1 is a description of power-spectrum transfer through a unity-gain linear filter (i.e. a convolution integral). As known from linear-systems analysis,<sup>19</sup> the power spectrum of a stochastic process in this case is passed via the MTF of the filter as shown in Table 1. The difference between noise-transfer through a linear filter and that through a stochastic scattering stage is fundamental to any analysis of medical imaging systems, and is a direct consequence of the discrete nature of image quanta. Stochastic amplification and scattering processes act on distributions of quanta only. No such restriction applies to deterministic blur processes.

## B. Early Application of the Cascaded Approach

One of the first applications of the cascaded approach examined the simplest case of nonlinear film-grain response; namely, that associated with a 2-quantum threshold.<sup>46,47</sup> Rabbani and Shaw showed that an exact solution was obtained for radiographic screen-film noise as a function of quantum exposure level and grain sensitivities, although under the assumption of a uniform checkerboard array of grains. Figure 5 shows a schematic of the radiographic screen-film model according to their assumptions. This approach was subsequently extended to a more complete analysis of screen-film systems,<sup>43,48</sup> including a detailed study of the effects of the depth-dependence of x-ray interactions on the MTF and noise-power spectrum of radiographic screens.<sup>49</sup> It was also extended to include the effect of a broad x-ray spectral width on the transfer of signal and noise in a screen-film system by allowing the average gain characterizing the amplification

stage (conversion to light) to be a random variable reflecting the distribution of x-ray energies.<sup>43</sup>

While the relationships in Table 1 describing photon signal and noise transfer were initially derived using a moment-generating approach, Barrett et al.<sup>45</sup> showed that the same results can be obtained very elegantly using statistical point-process theory, and Mulder<sup>50</sup> obtained similar results based on a variance approach. The transfer approach has since been applied and extended by several investigators in the analysis of medical imaging systems. For instance, Nishikawa and Yaffe<sup>51</sup> described a theoretical model of the NEQ and DQE in radiographic screens allowing for a distribution of x-ray interaction depths.

It is satisfying to note that intuitive theories and empiricisms that ignored the subtleties of photon noise transfer (for instance by representing image-blurring processes as linear filters rather than as stochastic scattering stages - hence leading to misleading predictions and interpretations of output/image power-spectra shapes) have at least partially subsided within medical imaging, although the reader should be aware that they still prevail elsewhere, for example in some multi-stage theories of SNR-transfer in electrophotography.

## C. DQE of Cascaded Systems

The concept of noise transfer through cascaded multi-stage systems with gain has been known for some time. Notably, Zwieg<sup>44</sup> described the effect of multi-stage gains in terms of the DQE in the nineteen-sixties. Using this approach, an imaging system is represented as a cascade of amplification-only stages, and the number of image quanta (per arbitrary resolving element such as an image pixel) is computed for each stage. If the cascaded amplification factor through each successive stage is always much greater than unity, the output SNR is determined only by the number of input quanta. However, if the cascaded amplification factor falls to less than unity at any stage, a bottleneck occurs that will degrade the output SNR. When this happens, this stage is sometimes referred to as the “quantum sink” of the system.

This type of analysis in imaging can be traced directly to Albert Rose. In the nineteen-forties, he published what is thought to be the first analysis of this type in which he assessed a video chain in a model that included the distribution of light quanta making up the original scene, the television pickup tube and lenses, video amplifiers and CRT display, and the retina in an observer. He plotted the number of image quanta at each stage and showed that two bottlenecks were predicted: one at the photo cathode of the pickup tube and the other at the photo surface of the retina.<sup>3</sup>

This “quantum accounting diagram” (QAD) analysis was subsequently performed routinely for many medical imaging systems<sup>52–56</sup> where system designers used this information to optimally choose gain parameters when matching components. It is known now from the binomial theorem that the DQE for an  $N$ -stage Zwieg-type cascaded model can be written approximately as

$$DQE = \frac{1}{1 + \frac{1}{g_1} + \frac{1}{g_1 g_2} + \dots + \frac{1}{g_1 g_2 \dots g_N}} \quad (23)$$

Elementary Process	$\bar{q}$ Transfer	$NPS(u)$ Transfer
Stochastic amplification	$\bar{q}_{out} = \bar{g}\bar{q}_{in}$	$NPS_{out}(u) = \bar{g}^2 NPS_{in}(u) + \sigma_g^2 \bar{q}$
Deterministic blur	$\bar{q}_{out} = \bar{q}_{in}$	$NPS_{out}(u) = NPS_{in}(u) MTF^2(u)$
Stochastic scattering	$\bar{q}_{out} = \bar{q}_{in}$	$NPS_{out}(u) = [NPS_{in}(u) - \bar{q}_{in}] MTF^2(u) + \bar{q}_{in}$

Table 1: Expressions describing transfer of average number of quanta,  $\bar{q}$ , and noise,  $NPS(u)$ , through three elementary processes.

where  $\bar{g}_j$  is the mean quantum gain of the  $j$ -th amplification stage. The product  $\bar{g}_1 \bar{g}_2 \dots \bar{g}_j$  gives the normalized number of quanta at the  $j$ -th stage, and is displayed graphically as a function of the stage number in a QAD analysis. Any stage with a product less than unity is a quantum sink and degrades the system DQE.

This result had great utility for “back-of-the-envelope” type calculations of the DQE, but it is now known this result is too simplistic and was responsible for much wasted effort in the development of some new designs by failing to predict quantum sinks at non-zero spatial frequencies. Even today, Eq. (23) is sometimes used to predict a high DQE for system designs that have no chance of success. The primary reason for this limitation is the fact that similar to the Rose model, this analysis shows only first-order statistics, and does not reflect spatial correlations in the image quanta. These correlations degrade the DQE at non-zero spatial frequencies.

This Zwieg-type model was generalized to include second-order statistics by Cunningham et al.<sup>57</sup> using the noise-transfer relationships of Rabbani et al.<sup>42</sup> They showed that the frequency-dependent DQE of a cascaded system consisting of amplification and scattering stages is described by

$$DQE(u) = \frac{1}{1 + \frac{1 + \epsilon_{g_1} MTF_1^2(u)}{\bar{g}_1 MTF_1^2(u)} + \dots + \frac{1 + \epsilon_{g_N} MTF_N^2(u)}{\bar{g}_1 \dots \bar{g}_N MTF_1^2(u) \dots MTF_N^2(u)}} \quad (24)$$

where  $\epsilon_{g_j}$  is the gain Poisson excess of the  $j$ -th stage given by

$$\epsilon_{g_j} = \frac{\sigma_{g_j}^2}{\bar{g}_j} - 1. \quad (25)$$

Poisson gain corresponds to a variance  $\sigma_{g_j}^2 = \bar{g}_j$  and excess  $\epsilon_{g_j} = 0$ . Deterministic gain (a gain with no random variability) corresponds to a variance  $\sigma_{g_j}^2 = 0$  and excess  $\epsilon_{g_j} = -1$ .  $MTF_j(u)$  is the MTF of the scattering process at the  $j$ -th stage. Each stage can represent only an amplification or scattering process, but not both. For amplification at the  $j$ -th stage,  $MTF_j(u) = 1$ . For a scattering  $j$ -th stage,  $\bar{g}_j = 1$  and  $\epsilon_{g_j} = -1$ . In practice, the excess terms are often small enough to be neglected and Eq. (24) then simplifies to

$$DQE(u) \approx \frac{1}{1 + \frac{1}{\bar{g}_1 MTF_1^2(u)} + \dots + \frac{1}{\bar{g}_1 \dots \bar{g}_N MTF_1^2(u) \dots MTF_N^2(u)}} \quad (26)$$

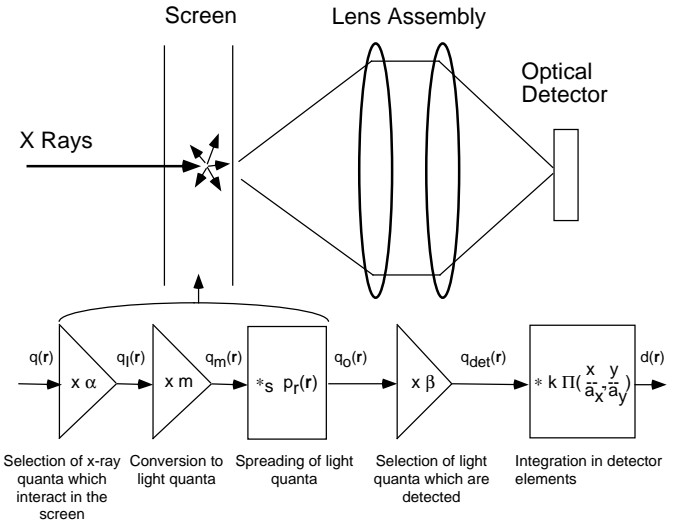


Figure 6: Schematic of a hypothetical system consisting of a radiographic screen, lens assembly and CCD camera.

which has a pleasing symmetry with Eq. (23) and is often sufficiently accurate for “back-of-the-envelope”-type calculations.

The Fourier-based Eq. (24) differs to the particle-based Eq. (23) in several respects. It shows that scattering stages can degrade the DQE dramatically when the MTF value drops with increasing spatial frequency. In fact, where Eq. (23) might predict that a minimum of approximately 10 quanta at each stage will easily prevent a secondary quantum sink, Eq. (24) shows that approximately 10 times that number is required at the frequency for which the MTF has a value of 0.3. Specific values will depend on system particulars, but it is clear that the frequency dependence of this type of analysis is critically important.

The Fourier-based QAD analysis provides a theoretical estimate of the DQE based only on the mean gain, gain variance, and scattering MTF of each stage - parameters that can generally be estimated or measured from an analysis of each stage independently. Equation (24) also establishes a direct theoretical relation between the frequency-dependent DQE and the number of primary or secondary image quanta at each stage. If any of the product terms of gains and squared scatter MTFs in the denominator of Eq. (24) are less than

### QUANTUM ACCOUNTING DIAGRAM

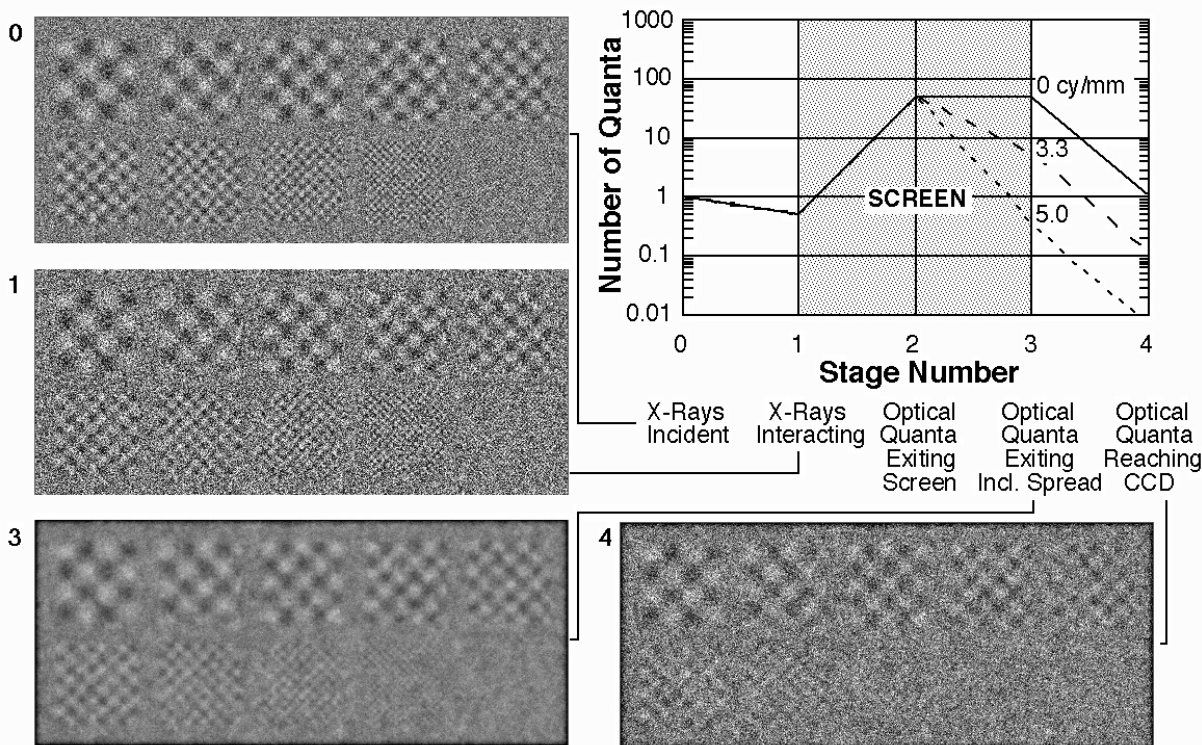


Figure 7: The “quantum accounting diagram” analysis of the system in Fig. 6 shows that a secondary quantum sink exists in the number of optical quanta at spatial frequencies greater than approximately 2.5 cycles/mm. A Monte Carlo calculation was used to generate images composed of the distribution of image quanta at each stage of the cascade, illustrating the degradation in image quality.

unity at any specified frequency, the DQE will be degraded. This result forms the basis for interpretation of a Fourier-based quantum sink concept that can be used to ensure that a sufficient number of quanta are present at each stage to adequately transfer the SNR for all spatial frequencies of interest.<sup>57</sup>

The visual appearance of a secondary quantum sink at non-zero frequencies is illustrated with a Monte Carlo calculation for the hypothetical imaging system illustrated in Fig. 6. The system consists of a radiographic screen, optical lens assembly, and CCD camera. Figure 7 shows the corresponding QAD analysis with simulated images corresponding to each stage in the cascaded model, demonstrating the deteriorating image quality.<sup>58</sup> In this example, a secondary quantum sink exists in the detected optical quanta at spatial frequencies greater than approximately 2.5 cycles/mm causing a loss of image SNR for the high-frequency patterns.

The practical utility of using the cascaded linear-systems approach has been demonstrated in recent studies of real systems. Figure 8 shows excellent agreement obtained between the experimentally measured DQE of a video-camera-based imaging system being developed by Munro et al. and the theoretical DQE generated with the cascaded linear-systems analysis by Bissonnette et al.<sup>59</sup> The system produces images using high-energy (several MeV) x rays from a linear accelerator. It uses a copper plate to generate electrons from the high-energy x rays which subsequently generate an optical image using a phosphor layer. The QAD analysis showed

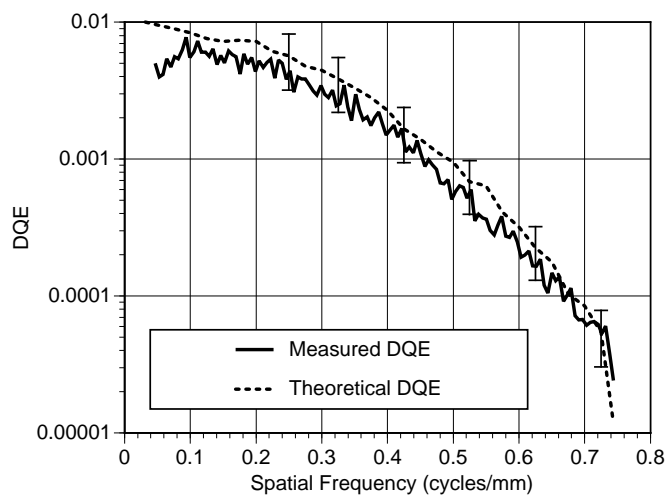


Figure 8: The experimentally measured DQE and the theoretical DQE based on the cascaded model show excellent agreement for a video-based imaging system developed for radiation therapy verification.

that output SNR was degraded by an inadequate number of light quanta being collected by the optical system at spatial frequencies above approximately 0.25 cycles/mm. Excellent agreement between theory and experiment was also obtained by Siewerdsen et al.<sup>60,61</sup> for an active matrix flat-panel imager being developed for digital radiography by Antonuk et al.<sup>60</sup>

#### D. Parallel Cascades

The cascaded models described so far have consisted of a single serial cascade of elementary processes, which is inadequate for the analysis of more complex systems in which the output signal consists of contributions from two or more processes. For example, non-zero cross-over film in a double-screen cassette is exposed to light coming from both the front and rear screens. If these parallel processes are statistically independent of each other, the output NPS may be simply a sum of the output NPS from each process. However, when the processes are not statistically independent, it has been shown by Cunningham<sup>62</sup> that is necessary to include appropriate cross-spectral density terms in the cascaded model. An example of this problem occurs in the analysis of reabsorption of characteristic radiation generated within an imaging detector such as a radiographic screen, where light is emitted at both the primary x-ray interaction and reabsorption sites.

Reabsorption will occur at a random location according to some probability density distribution near the primary interaction, adding a statistical correlation to the image quanta and hence an additional spatial-frequency dependence to the NPS. These considerations can be important in many imaging detectors, including x-ray image intensifiers, computed radiography systems and flat-panel active matrix array digital detectors of various designs, and can be incorporated into a cascaded model as illustrated in Fig. 9. The single input (representing a single incident quantum) splits into three parallel cascades corresponding to paths A, B and C in Fig. 9, representing three possible sequences of events whereby light is generated in the screen: A) light generated at the primary interaction site when no characteristic K x ray is emitted; B) light generated at the primary site when a characteristic K x ray is emitted; and, C) light generated at the reabsorption site. Cascades A and B are connected through "stochastic branch points" which, for each interaction, determines an outcome "yes" or "no" where "yes" is obtained randomly with the specified probability and "no" otherwise. Light emitted from the screen is the sum of contributions from each path. The corresponding NPS is the sum of the NPS from each of the three serial cascades plus the cross-spectral density terms. In this case, the effect of the cross term was to increase the NPS (and decrease the DQE) at spatial frequencies below approximately 2 cycles/mm by up to 10%.

Reabsorption was studied prior to use of the cascaded model, but required a more complex statistical analysis. For instance, Metz and Vyborny<sup>63</sup> looked at the same radiographic screen and obtained the same result, and Hillen<sup>64</sup> has examined reabsorption in an x-ray image intensifier.

#### E. Digital Imaging Systems

The use of digital imaging systems is now well established clinically. However, the theoretical tools required to describe effects such as noise aliasing or a non-unity detector fill factor remain surprisingly elusive and misused. While the cascaded linear-systems approach can be used to describe these digital systems,<sup>28,65</sup> care must be taken to properly handle the mathematical infinities and generalized functions which may arise, and to make proper use of the discrete Fourier transform as a representation of the Fourier transform integral. As noted earlier, the Fourier approach assumes shift-invariant imaging systems and WSS noise processes. Barrett et al.<sup>66,67</sup> have recently described methods such as the Fourier crosstalk matrix which provide a direct mapping of the continuous image space to digital image data, and do not require shift invariance or WSS noise processes. These approaches may provide additional insight in the future, particularly for the analysis of digital imaging systems.

#### V. CONCLUSIONS

The theoretical representation of signal and noise in medical diagnostic imaging has undergone a revolution so far as a general approach is concerned. The authors have attempted to illustrate this primarily from the viewpoint of screen-film systems, where a community concerned mainly with sensitometry and densitometry has given way to one focused around modern SNR-based imaging theory, and early particle-based models of noise pioneered by Rose have been extended by linking to more comprehensive Fourier-based models. The development of screen-film systems has reached the stage where further advances within tightly-bound constraints of quantum efficiency, speed, and image quality are not far from those set by the bounds of physics, as opposed to the bounds of technology. Indeed, incremental but important advances in performance now come mainly from the insight cast by fundamental analysis and evaluation afforded by modern imaging theory. A further important factor is due to the parallel development of competing technologies, especially in the digital domain. A broad-based information-theoretic imaging theory has thus been essential so that those concerned with all technologies might continue their dialogue within a general language. In this context it is worth emphasizing the point that far from being a passing fashion, the major parts of this theory have been in place for almost half a century. Those who came before - including Al Rose and his contemporaries - laid a solid foundation, and those in modern times concerned with transferring this knowledge to the field of medical diagnostic imaging have had a relatively straightforward task.

#### VI. REFERENCES

1. American National Standards Institute, "Methods for the Sensitometry of Medical X-Ray Screen-Film Processing Systems", ANSI Publication PH.2.43-1982 (American National Standards Institute, New York, 1998).
2. A. Rose, "Sensitivity performance of the human eye on

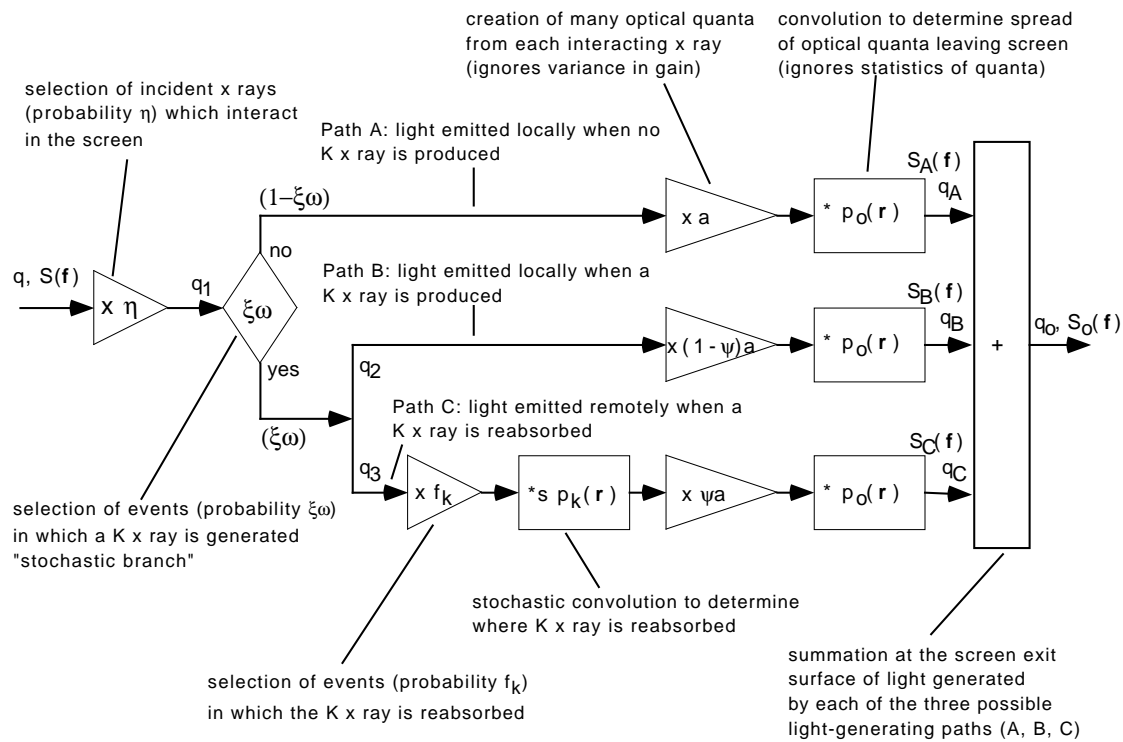


Figure 9: Schematic illustration of the parallel cascade model used to determine the reabsorption of characteristic K x-rays in a radiographic screen.

an absolute scale," J Opt Soc Am 38, 196-208 (1948).

3. A. Rose, "Television pickup tubes and the problem of vision," in *Advances in Electronics and Electron Physics*, edited by Marston (Academic Press, New York, 1948), pp. 131-166.

4. P.B. Fellgett, "On the ultimate sensitivity and practical performance of radiation detectors," J Opt Soc Am 39, 970 (1949).

5. H.J. Zweig, "Performance criteria for photo-detectors - concepts in evolution," Photo Sc Eng 8, 305 (1964).

6. R.C. Jones, "A new classification system for radiation detectors," J Opt Soc Am 39, 327 (1949).

7. A. Rose, "Quantum and noise limitations of the visual process," J Opt Soc Am 43, 715-716 (1953).

8. A.E. Burgess, "The Rose Model - Revisited," J Opt Soc Am A (1999) [In Press].

9. K. Rossmann, "Measurement of the modulation transfer function of radiographic systems containing fluorescent screens," Phys Med Biol 9, 551-557 (1964).

10. K. Doi, "Optical transfer functions of the focal spot of x-ray tubes," Am J Roentgenol 94, 712-718 (1965).

11. G. Lubberts and K. Rossmann, "Modulation transfer function associated with geometrical unsharpness in medical radiography," Phys Med Biol 12, 65-77 (1967).

12. K. Rossmann and G. Sanderson, "Validity of the modulation transfer function of radiographic screen-film systems measured by the slit method," Phys Med Biol 13, 259-268 (1968).

13. K. Rossmann, "The spatial frequency spectrum: A means for studying the quality of radiographic imaging systems," Radiology 90, 1-13 (1968).

14. K. Rossmann, "Point Spread-Function, Line Spread-

Function, and Modulation Transfer Function," Radiol 93, 257-272 (1969).

15. "Modulation Transfer Function of Screen-Film Systems", ICRU Report 41 (International Commission on Radiation Units and Measurements, Bethesda, 1986).

16. A.E. Burgess, "Focal spots: I. MTF separability," Invest Radiol 12, 36-43 (1977).

17. A.E. Burgess, "Focal spots: II. Models," Invest Radiol 12, 44-53 (1977).

18. C.E. Metz and K. Doi, "Transfer function analysis of radiographic imaging systems," Phys Med Biol 24, 1079-1106 (1979).

19. J.D. Gaskill, *Linear Systems, Fourier Transforms, and Optics*, (John Wiley & Sons, New York, 1978).

20. J.C. Dainty and R. Shaw, *Image Science*, (Academic Press, New York, 1974).

21. H.H. Barrett and W. Swindell, *Radiological Imaging - The Theory of Image Formation, Detection, and Processing*, (Academic Press, New York, 1981).

22. M.C. Steckner, D.J. Drost and F.S. Prato, "Computing the modulation transfer function of a magnetic resonance imager," Med Phys 21, 483-498 (1994).

23. A. Rose, "A unified approach to the performance of photographic film, television pick-up tubes, and the human eye," J Soc Motion Pict Telev Eng 47, 273-294 (1946).

24. A. Rose, *Vision: Human and Electronic*, (Plenum Press, New York, 1974).

25. R.F. Wagner and K.E. Weaver, "Noise measurements on rare-earth intensifying screen systems," in *Medical X-Ray Photo-Optical Systems Evaluation*, edited by R.F. Wagner, K.E. Weaver and D.G. Goodenough, Proc SPIE 56:198-207 (1974).

26. O.H. Schade, "Evaluation of noisy images," in Medical X-Ray Photo-Optical Systems Evaluation, edited by R.F. Wagner, K.E. Weaver and D.G. Goodenough, Proc SPIE 56:107-114 (1974).
27. A. Papoulis, Probability, random variables, and stochastic processes, 3 Ed. (McGraw Hill, New York, 1991).
28. I.A. Cunningham, "Analyzing System Performance," in The Expanding Role of Medical Physics in Diagnostic Imaging, edited by G.D. Frey and P. Sprawls (Advanced Medical Publishing for American Association of Physicists in Medicine, Madison, Wisconsin, 1997), pp. 231-263.
29. R. Shaw, "The equivalent quantum efficiency of the photographic process," J Photogr Sc 11, 199-204 (1963).
30. "Medical Imaging - The Assessment of Image Quality", ICRU Report 54 (International Commission of Radiation Units and Measurements, Bethesda, 1995).
31. C.E. Metz, R.F. Wagner, K. Doi, D.G. Brown, R.M. Nishikawa and K.J. Myers, "Toward consensus on quantitative assessment of medical imaging systems. [Review]," Med Phys 22, 1057-1061 (1995).
32. J.T. Dobbins, D.L. Ergun, L. Rutz, D.A. Hinshaw, H. Blume and D.C. Clark, "DQE(f) of four generations of computed radiography acquisition devices," Med Phys 22, 1581-1593 (1995).
33. R. Shaw, "Some fundamental properties of xeroradiographic images," in Application of Optical Instrumentation in Medicine IV, edited by J.E. Gray and W.R. Hendee, Proc SPIE 70:359-363 (1975).
34. R.F. Wagner and E.P. Muntz, "Detective quantum efficiency (DQE) analysis of electrostatic imaging and screen-film imaging in mammography," in Application of Optical Instrumentation in Medicine VII, edited by J.E. Gray, Proc SPIE 173:162-165 (1979).
35. R. Shaw and R.L. Van Metter, "An analysis of the fundamental limitations of screen-film systems for x-ray detection I. General theory," in Application of Optical Instrumentation in Medicine XII, edited by R.H. Schneider and S.J. Dwyer, Proc SPIE 454:128-132 (1984).
36. R. Shaw and R.L. Van Metter, "An analysis of the fundamental limitations of screen-film systems for x-ray detection II. Model calculations," in Application of Optical Instrumentation in Medicine XII, edited by R.H. Schneider and S.J. Dwyer, Proc SPIE 454:133-141 (1984).
37. P.C. Bunch, R. Shaw and R.L. Van Metter, "Signal-to-noise measurements for a screen-film system," in Application of Optical Instrumentation in Medicine XII, edited by R.H. Schneider and S.J. Dwyer, Proc SPIE 454:154-163 (1984).
38. R. Shaw and R.L. Van Metter, "The role of screen and film in determining the noise-equivalent number of quanta recorded by a screen-film system," in Application of Optical Instrumentation in Medicine XIII, edited by R.H. Schneider and S.J. Dwyer, Proc SPIE 535:184-194 (1985).
39. P.C. Bunch, K.E. Huff, R. Shaw and R.L. Van Metter, "Comparison of theory and experiment for the DQE of a radiographic screen-film system," in Application of Optical Instrumentation in Medicine XIII, edited by R.H. Schneider and S.J. Dwyer, Proc SPIE 535:166-185 (1985).
40. R.L. Van Metter and R. Shaw, "The effect of bias exposure on the detective quantum efficiency of radiographic screen-film systems," in Application of Optical Instrumentation in Medicine XIII, edited by R.H. Schneider and S.J. Dwyer, Proc SPIE 535:157-162 (1985).
41. P.L. Dillon, J.F. Hamilton, M. Rabbani, R. Shaw and R.L. Van Metter, "Principles governing the transfer of signal modulation and photon noise by amplifying and scattering mechanisms," in Application of Optical Instrumentation in Medicine XIII, edited by R.H. Schneider and S.J. Dwyer, Proc SPIE 535:130-139 (1985).
42. M. Rabbani, R. Shaw and R.L. Van Metter, "Detective quantum efficiency of imaging systems with amplifying and scattering mechanisms," J Opt Soc Am A 4, 895-901 (1987).
43. M. Rabbani and R.L. Van Metter, "Analysis of signal and noise propagation for several imaging mechanisms," J Opt Soc Am A 6, 1156-1164 (1989).
44. H.J. Zweg, "Detective quantum efficiency of photodetectors with some amplifying mechanism," J Opt Soc Am 55, 525-528 (1965).
45. H.H. Barrett, R.F. Wagner and K.J. Myers, "Correlated point processes in radiological imaging," in Medical Imaging 1997: Physics of Medical Imaging, edited by R.L. Van Metter and J. Beutel, Proc SPIE 3032:110-125 (1997).
46. M. Rabbani and R. Shaw, "The influence of grain threshold on quantum mottle in radiographic film-screen systems," in Medical Imaging, edited by S.J. Dwyer and R.H. Schneider, Proc SPIE 767:226-235 (1987).
47. M. Rabbani and R. Shaw, "The influence of grain threshold on quantum mottle in radiographic screen-film systems II," in Medical Imaging II: Part A-Image Formation, Detection, Processing, and Interpretation, edited by R.H. Schneider and S.J. Dwyer, Proc SPIE 914A:117-127 (1988).
48. M. Rabbani and R.L. Van Metter, "Some new applications of multivariate moment-generating functions to screen-film systems," in Medical Imaging III: Image Formation, edited by S.J. Dwyer, R. Jost and R.H. Schneider, Proc SPIE 1090:86-94 (1989).
49. R.L. Van Metter and M. Rabbani, "Analysis of the effects of depth dependence of x-ray interactions on the NPS of radiographic screens," in Medical Imaging IV: Image Formation, edited by R.H. Schneider, Proc SPIE 1231:271-274 (1990).
50. H. Mulder, "Signal and noise transfer through imaging systems consisting of a cascade of amplifying and scattering processes," J Opt Soc Am A 10, 2038-2045 (1993).
51. R.M. Nishikawa and M.J. Yaffe, "Model of the spatial-frequency-dependent detective quantum efficiency of phosphor screens," Med Phys 17, 894-904 (1990).
52. M.M. Ter-Pogossian, The physical aspects of diagnostic radiology, (Harper & Row, New York, 1967).
53. C.A. Mistretta, "X-ray image intensifiers," in AAPM No 3 The physics of medical imaging: recording system measurements and techniques, edited by A.G. Haus (American Institute of Physics, New York, 1979), pp. 182-205.
54. A. Macovski, Medical Imaging Systems, (Prentice-Hall, Inc., Englewood Cliffs, N.J., 1983).
55. H. Roehrig, S. Nudelman and T.Y. Fu, "Electro-optical devices for use in photoelectronic-digital radiology," in AAPM No. 11 Electronic Imaging in Medicine, edited by G.D. Fullerton, W.R. Hendee, J.C. Lasher, W.S. Properzio and S.J. Riederer (American Institute of Physics, New York, 1984), pp. 82-129.

56. H. Roehrig and T.Y. Fu, "Physical properties of photoelectronic imaging devices and systems," in AAPM No 12 Recent developments in digital imaging, edited by K. Doi, L. Lanzl and P.J.P. Lin (American Institute of Physics, New York, 1985), pp. 82-140.
57. I.A. Cunningham, M.S. Westmore and A. Fenster, "A spatial-frequency dependent quantum accounting diagram and detective quantum efficiency model of signal and noise propagation in cascaded imaging systems," *Med Phys* 21, 417-427 (1994).
58. I.A. Cunningham, M.S. Westmore and A. Fenster, "Visual impact of the non-zero spatial frequency quantum sink," in *Medical Imaging 1994: Physics of Medical Imaging*, edited by R. Shaw, Proc SPIE 2163:274-283 (1994).
59. J.P. Bissonnette, I.A. Cunningham, D.A. Jaffray, A. Fenster and P. Munro, "A quantum accounting and detective quantum efficiency analysis for video-based portal imaging," *Med Phys* 24, 815-826 (1997).
60. J.H. Siewerdsen, L.E. Antonuk, Y. El-Mohri, J. Yorkston, W. Huang, J.M. Boudry and I.A. Cunningham, "Empirical and theoretical investigation of the noise performance of indirect detection, active matrix flat-panel imagers (AMFPIs) for diagnostic radiology," *Med Phys* 24, 71- 89 (1997).
61. J.H. Siewerdsen, L.E. Antonuk, Y. El-Mohri, J. Yorkston, W. Huang and I.A. Cunningham, "Signal, noise power spectrum and detective quantum efficiency of indirect-detection flat-panel imagers for diagnostic radiology," *Med Phys* 25, 614-628 (1998).
62. I.A. Cunningham, "Linear-systems modeling of parallel cascaded stochastic processes: The NPS of radiographic screens with reabsorption of characteristic radiation," in *Medical Imaging 1998: Physics of Medical Imaging*, edited by J.T. Dobbins and J.M. Boone, Proc SPIE 3336:220- 230 (1998).
63. C.E. Metz and C.J. Vyborny, "Wiener spectral effects of spatial correlation between the sites of characteristic x-ray emission and reabsorption in radiographic screen-film systems," *Phys Med Biol* 28, 547-564 (1983).
64. W. Hillen, W. Eckenbach, P. Quadflieg and T. Zaengel, "Signal-to-noise performance in cesium iodide x-ray fluorescent screens," in *Medical Imaging V: Image Physics*, edited by R.H. Schneider, Proc SPIE 1443:120-131 (1991).
65. I.A. Cunningham, "Degradation of the detective quantum efficiency due to a non-unity detector fill factor," in *Medical Imaging 1997: Physics of Medical Imaging*, edited by R.L. Van Metter and J. Beutel, Proc SPIE 3032:22-31 (1997).
66. H.H. Barrett, J.L. Denny, R.F. Wagner and K.J. Myers, "Objective assessment of image quality II: Fisher information, Fourier crosstalk and figures of merit for task performance," *J Opt Soc Am A* 12, 834-852 (1995).
67. H.H. Barrett, J.L. Denny, H.C. Gifford, C.K. Abbey, R.F. Wagner and K.J. Myers, "Generalized NEQ: Fourier analysis where you would least expect to find it," in *Medical Imaging 1996: Physics of Medical Imaging*, edited by R.L. Van Metter and J. Beutel, Proc SPIE 2708:41-52 (1996).